American Journal of Pathology, Vol. 144, No. 3, March 1994

Extracellular Signal Regulated Kinases

Localization of Protein and mRNA in the Human Hippocampal Formation in Alzheimer's Disease

Bradley T. Hyman, Ted E. Elvhage, and Joell Reiter

From the Neurology Service, Massachusetts General Hospital and Harvard Medical School, Boston, Massachusetts

MAP kinases (MAPK) are a family of serine/threonine (Ser/Thr) kinases that link cell surface signals to changes in enzyme activity and gene expression. They are the products of the newly described gene family referred to as extracellular signal regulated kinases (ERKs). Moreover, MAPKs phosphorylate tau in vitro at Ser/Thr Proline sites, generating a multiply phosphorylated tau protein that is similar to the hyperphosphorylated tau found in Alzheimer neurofibrillary tangles (NFTs). We studied MAPK immunoreactivity and in situ hybridization patterns of the two major genes that comprise MAPK activity, ERK1 and ERK2, in the human hippocampal formation. Our goal was to determine whether the pattern of ERK expression is consistent with the hypothesis that MAPKs contribute to NFT formation. ERK1 mRNA is present in small amounts and confined primarily to dentate gyrus granule cells. ERK2 mRNA, by contrast, gives a much stronger hybridization signal and is present in dentate gyrus granule cells and pyramidal cells throughout all hippocampal subfields and adjacent temporal neocortex. Quantitative measures of ERK2 mRNA reveal that NFT-bearing neurons contain approximately 15% less ERK2 mRNA than nearest neighbors that do not contain NFT. NFT-bearing neurons contain approximately 25% less polyA mRNA, suggesting a relative preservation of ERK2 mRNA even in metabolically compromised cells. MAPK immunoreactivity (which represents both ERK1 and ERK2) is seen in neuronal soma, dendrites, axons, and in reactive astrocytes. In Alzheimer's disease, neurons that contain NFTs are also MAPK immunoreactive, but neurons that contain the highest amounts of MAPK immunoreactivity are not necessarily vulnerable for NFT. MAPK immunoreactivity is present in the same neurons as NFT and in the same subcellular compartments as tau, supporting a role for MAPKs in tau phosphorylation in Alzheimer's disease. However, the presence of ERK immunoreactivity is not sufficient to predispose neurons to NFT formation. (Am J Pathol 1994, 144:565–572)

The major biochemical component of neurofibrillary tangles (NFTs) in Alzheimer's disease (AD) is a hyperphosphorylated form of the microtubule-associated protein tau.[1] Because NFT formation appears to be a key feature of the pathophysiology of AD,[2] intensive study is directed at understanding the conversion of tau into NFT. Phosphorylated tau derived from the paired helical filaments (PHF) that make up NFT differs from normal tau isolated from brain in two distinct ways: it has a higher apparent molecular weight on Western blots and it possesses unique antigenic recognition sites recognized by several anti-tau or anti-NFT antibodies. Furthermore, phosphorylated tau changes its conformation and interacts less strongly with microtubules.[3] *In vitro*, tau can be phosphorylated by several protein kinases, including protein kinase C, casein kinase II, calcium/calmodulin-dependent protein kinase II, cAMP-dependent protein kinase,[4–6] glycogen synthase kinase 3,[7,8] and MAP kinases (MAPK; also referred to as mitogen-activated or MAP-2 kinases).[9–12] It is unknown which if any of these lead to phosphorylation of tau in NFTs *in vivo*. Of the kinases examined, however, only the MAPKs and glycogen synthase kinase

Supported by NIH AG08487, the Alzheimer Association, and the Brookdale Foundation.

Accepted for publication October 22, 1993.

Address reprint requests to Dr. Bradley T. Hyman, Neurology Service, Warren 408, Massachusetts General Hospital, Boston, MA 02114.

3 phosphorylate tau in such a way as to cause both a PHF taulike shift in electrophoretic mobility and recognition by a panel of PHF-tau antibodies.

Extracellular signal regulated kinases (ERKs) are a recently cloned gene family of kinases that have MAPK activity, are activated by a wide variety of extracellular signals, and are a common feature of the tyrosine kinase receptor and heterotrimeric G protein cascades. They have been implicated in cell cycling, response to insulin and growth factors, and response of neurons to neural activity.[13–15] They appear to be central players in kinase cascades that link cell surface stimulation to changes in enzyme activity and gene expression.[16–18] Despite a rapidly expanding literature on the biochemical and physiological properties of these kinases, little anatomic data are available concerning their localization in brain.

If ERKs are fundamentally involved in tau phosphorylation in Alzheimer brain, it is crucial that they are present in the same location and cell types that develop NFT. Neuropathological studies[19,20] have shown that a subpopulation of pyramidal neurons within the CA1/subicular area are the neurons within the hippocampus most at risk for developing NFT, and essentially all cases of AD predictably contain NFT in these neurons. This study used *in situ* hybridization and immunohistochemistry to determine the anatomical distribution of the MAPKs ERK1 and ERK2 in the human hippocampal formation and examine in which cellular compartments they reside. Furthermore, we asked whether they are present in the population of neurons affected by NFT and tested the possibility that expression of these kinases is increased in neurons that develop NFT.

Materials and Methods

Twelve individuals were studied. Seven had the clinical and neuropathological diagnoses of AD (1 of whom had trisomy 21, 2 had concurrent Parkinson's disease, and 1 had concurrent diffuse Lewy body disease, mean age 76.7 years, range 61 to 96 years, postmortem interval 12.1 ± 7.8 hours). Five were neurologically normal control individuals who did not meet Khachaturian criteria for AD by neuropathological evaluation (mean age 57.4 years, range 22 to 77 years postmortem interval 27.6 ± 15.8 hours). All neuropathological evaluations were conducted independently by the Alzheimer Disease Brain Bank using the Bielchowski silver stain for senile plaques and NFTs. Anatomical analyses were performed without knowledge of the age or diagnostic category.

Immunohistochemistry

The material studied here consisted of the hippocampal formation and adjacent temporal neocortex that had been fixed in paraformaldehyde-lysine-metaperiodate at 4 C for 24 to 48 hours then cryoprotected at 4 C in 15% glycerol/0.1 M phosphate-buffered saline (pH 7.4) for an additional 24 hours. Fifty-micron thick sections were cut on a freezing sledge microtome. Sections were processed for immunohistochemistry using a free floating procedure. ERK immunoreactivity was identified using a monoclonal antibody (Zymed clone Z033) raised against a synthetic peptide representing 21 amino acid sequence near the carboxyl terminus of MAPK leading to reactivity with both ERK1 and ERK2.[21] Immunoreactivity was detected using a goat anti-mouse peroxidase-linked secondary antibody (Jackson Immunoresearch, West Grove, PA) and visualized with diaminobenzidine. Some sections were lightly counterstained with thionin to aid in cellular identification and in determining cytoarchitectural fields. Control tissue was incubated without primary antibody. For the double staining experiments, immunoreactivity was visualized using a rhodamine-linked secondary antibody and sections were counterstained with thioflavine S to detect NFT.

Quantitation of Immunohistochemical Product

Diffuse density measurement of the dentate gyrus and CA1/subicular area were obtained using a Leitz Aristoplan microscope equipped with stage encoders and a CCD-72 Dage-MTI video camera. Digitized information was used by the Bioquant Microquant Image Analysis System running on a Grafitica 486 computer. The dentate gyrus granule cell layer and the CA1/subicular field were outlined on each captured image by the operator and the area and optical density were measured. This was repeated on adjacent fields until the entire structure had been observed and a weighted average optical density calculated. The optical density was converted to diffuse density units (a negative log function) according to a conversion equation generated using a series of standard grey-scale (Kodak, Rochester, NY) as previously described.[22] Comparison of AD and control values was by Student's *t*-test.

In situ *Hybridization*

Fifty-micron thick sections of frozen tissue were cut on a sliding microtome and mounted on poly-L-

lysine-dipped slides. The tissue is treated with 24 U/ml pronase for 10′ at room temperature then washed in buffered saline and alcohol and allowed to dry. The 45 nucleotide long DNA probes were synthesized on an Applied Biosciences Oligonucleotide Synthesizer. Three probes were used: POLY TTTTTTTTTTTTTTTTTTTTTTTTTTTTTTTTTTTTTTTTT, ERK1 GGGGCAGCCAGAACCCCTTCCATTCCAAAACTGCCAGAGACTGGGA, and ERK2 CCGATGTCTGAGCACGTCCAGTCCTCTGAGCCCTTGTCCTGACAA.

The ERK1 and ERK2 probes were chosen from the 3′ untranslated region of the mRNA because of extensive homology within the coding region. Each probe was radiolabeled with ^{35}S-dATP (1000 to 3000 Ci/mmol) using Dupont's terminal transferase oligonucleotide 3′ end labeling kit. Approximately 3.6×10^6 counts of labeled probe in 120 μl hybridization solution (50% formamide, 10 mM Tris, 1 mM EDTA, 0.3 M NaCl, 10% dextran sulfate, 1× Denhardt solution, and 0.1 M DTT) was hybridized to mounted tissue at 37 C overnight. After hybridization, tissue is washed under increasingly stringent conditions, from 2× standard saline citrate (SSC) at room temperature to 0.5× SSC at 50 C. After rinsing in 70% ethanol the slides were air-dried and exposed to Amersham Hyperfilm BMax from 2 days to 6 weeks in a light-tight cassette with 14C standards (for quantitation of signal). Thereafter, sections were dipped in Kodak NTB2 emulsion, exposed for 1 to 2 weeks (poly-T) or 1 to 2 months (ERK1 and ERK2), developed, and counterstained with thioflavine S (for fluorescence detection of NFT and senile plaque) and lightly with thionin for cell bodies. Controls included pretreatment with RNAse (which obliterates all signal) and addition of 10-fold excess of unlabeled probe which also essentially eliminates all signal (Figure 1).

Quantitation of In Situ *Product*

A combination of bright field and fluorescent images provides the ability to demarcate neurons that contain or do not contain NFT. The Nissl counterstain was effectively removed from the black and white video image by introducing a Kodak 47B blue filter into the light path. The location of NFT is noted by inserting the fluorescent cubes in or out of the light path.[23] The density of *in situ* hybridization product (silver grains) is then measured in neurons that contain an NFT and in a nearest neighbor that is NFT-free. These measurements were conducted in the CA1 field for ERK2 (5 cases) and poly A (6 cases) probes. The ERK1 *in situ* product was sparse in CA1 and measurements were not thought to be meaningful. Approximately 15 pairs within each case were obtained; a single average diffuse density from each case was then used for further statistical analysis. Because these data were within case and field comparisons, no additional external corrections were applied.

Results

Figure 1 shows the overall pattern of ERK immunoreactivity in the hippocampal formation. The regional distribution was consistent in all cases, with no difference observed between AD and control cases. The most intensely stained area was the dentate gyrus granule cell layer, followed by CA3 and the mossy fiber zone, CA4, subiculum, then CA1. Many but not all neuronal cell bodies as well as many dendrites and axons in the neuropil were intensely immunoreactive. Presumed interneurons in stratum radiatum and in the deep white matter also stain intensely. In temporal neocortex, ERK immunoreactivity showed a laminar distribution with small pyramidal neurons in layers II and VI > moderate

Figure 1. *ERK immunoreactivity in the human hippocampal formation of a 77-year-old control individual (top) and an 85-year-old individual with Alzheimer disease (bottom). The dentate gyrus and CA3 areas are most heavily immunoreactive, although many neurons in all hippocampal subfields are stained.*

and large pyramidal neurons in layers III and V > layer IV. The large modified pyramidal neurons in layer II and those in layer IV of entorhinal cortex were also well stained.

To address the question of whether there was a change in the amount of ERK immunoreactivity in areas prone to NFT formation (CA1/subiculum) compared with areas that are relatively unaffected in AD (dentate gyrus), we measured the optical density of ERK immunoreactivity in the CA1/subiculum field and in the dentate gyrus granule cell layer using a Bioquant computerized image analysis system. There was no difference in the amount of ERK immunoreactivity in either the dentate gyrus (0.36 ± 0.03 optical density units AD; 0.39 ± 0.09 control, mean ± SE, not significant) or in the CA1/subicular field (0.27 ± 0.02 diffuse density units, AD; 0.30 ± 0.05 control, mean ± SE, not significant).

At higher magnification (Figure 2), the subcellular distribution of ERK immunoreactivity in pyramidal neurons in CA1 can be clearly seen. The neuronal soma and axons are immunoreactive, along with fine dendritic arborizations of both the apical and basilar dendrites. Increased staining in the nucleus was apparent in rare neurons but most frequently the neuronal nuclei were unstained. In addition to this population of neurons, reactive astrocytes were also immunoreactive. These were scattered throughout the hippocampal formation, primarily in AD, and were prominent also in temporal neocortex, especially in the infragranular layers and at the grey/white junction.

To determine whether or not ERK immunoreactivity co-localized within NFT-bearing neurons, we used a double immunofluorescence protocol visualizing ERK immunoreactivity with a rhodamine-linked secondary antibody and visualizing NFT with the fluorescent histochemical stain, thioflavine S. NFT-bearing neurons consistently contained ERK immunoreactivity (Figure 3), although NFTs themselves were not immunoreactive and extracellular or "tombstone" NFT were not associated with ERK staining.

In situ hybridization (Figure 4) was conducted to differentiate ERK1 and ERK2 patterns of anatomic distribution because the antibody should recognize both. The autoradiograms show that ERK1 mRNA is localized primarily in the dentate gyrus granule cells, and there is little ERK1 mRNA present in the hippocampal pyramids. By contrast, the ERK2 signal is extremely strong in the dentate gyrus granule cell layer and in CA4, CA3, CA1, and the subicular fileds. In addition, adjacent parahippocampal gyrus and temporal neocortex showed much stronger ERK2 than ERK1 hybridization in neurons. We con-

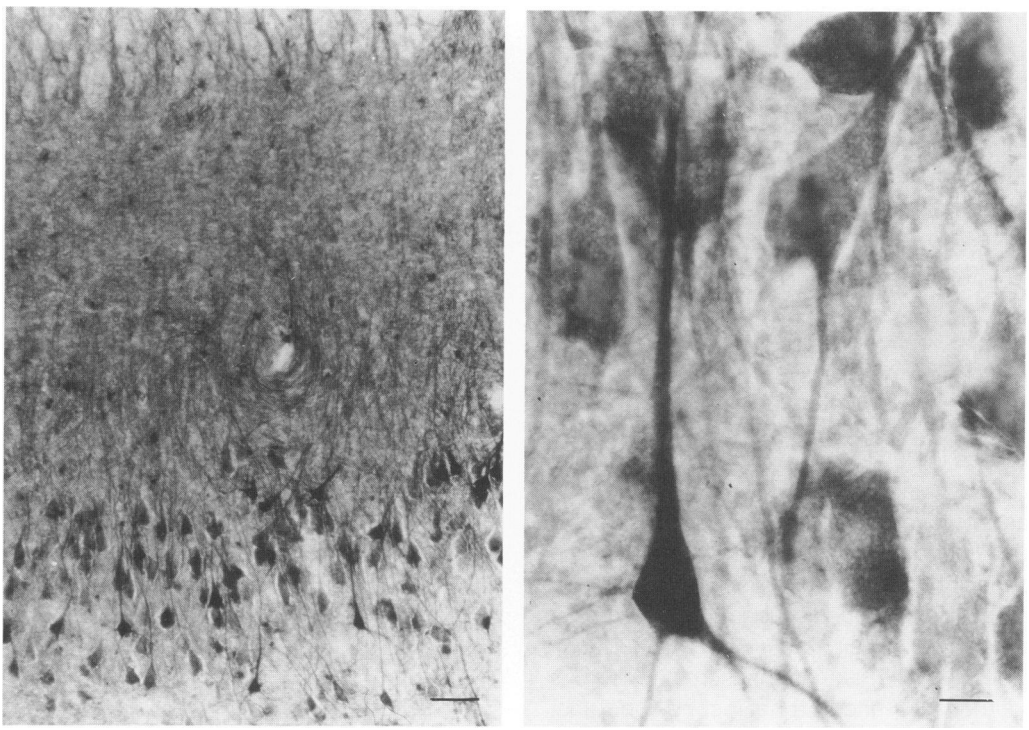

Figure 2. *Higher magnification of ERK (left) immunoreactivity in the CA1 area of the human hippocampus. Bar = 50 μm. Under ×100 magnification, ERK immunostaining (right) is clearly seen in the neuronal soma, dendrites, and axon. Bar = 10 μm.*

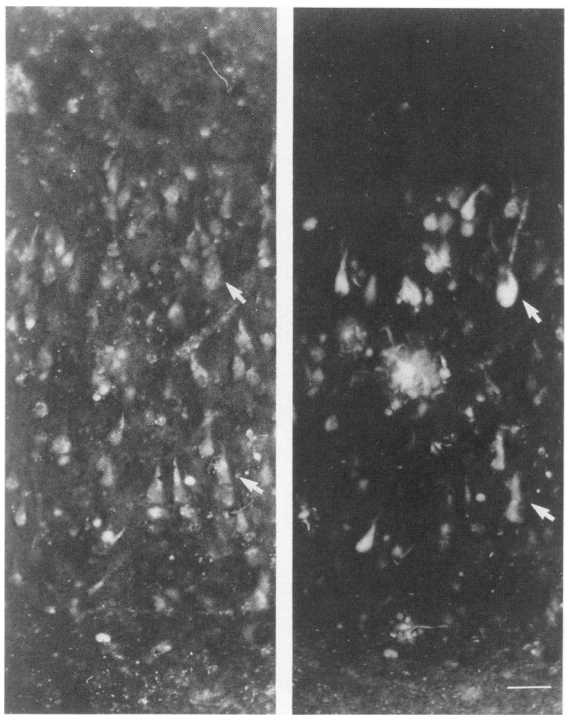

Figure 3. *Rhodamine immunofluorescence shows many ERK immunoreactive neurons in CA1 of an Alzheimer individual (left). The same field using barrier filters specific for thioflavine S reveals NFT and a senile plaque (right). NFT co-localize within ERK immunoreactive neurons. Bar = 40 μm.*

clude that the majority of the immunoreactivity we observed was due to ERK2.

Because the MAPK immunoreactivity was present throughout the cell bodies and neuropil, we measured regional levels and found no difference between control and AD brain. This technique is not well suited to ask the question about the individual neuron that contains or does not contain an NFT. This latter question was addressed by quantitating the ERK2 *in situ* hybridization product within NFT-bearing or nearest neighbor non-NFT-bearing neurons. This within-sample comparison obviates issues of differences in postmortem time, perimortem conditions, and technical issues of labeling probes, exposure times, and development of emulsion that can complicate quantitative comparison of *in situ* hybridization product between cases.[23] The diffuse density of hybridization product for ERK2 in NFT-bearing neurons was 0.85 ± 0.025% of non-NFT-bearing nearest neighbors ($P < 0.003$, paired *t*-test). For comparison, the same protocol was conducted using a poly-T probe to assess loss of poly-A mRNA in NFT-bearing neurons, yielding a value of 0.75 ± 0.04% ($P < 0.0015$).

Discussion

Several members of the ERK family of genes have been cloned, including ERK1 (p43), ERK2 (p42), and ERK3.[14] ERKs include the pp42 MAPK protein[13,15,24] that is one of the major tyrosine phosphorylated proteins in transformed cells and implicated in signal transduction. As assessed by Northern blots, ERKs are expressed in a developmentally and regionally specific fashion in brain[14] but the cell types and anatomic profile of expression of these genes is unknown.

ERK activity is regulated by dual phosphorylations at adjacent tyrosine and threonine sites.[25,26] A MAPK kinase, MEK, phosphorylates ERKs and thereby activates them.[27] In turn, MEK is phosphorylated by either a MEK kinase or Raf, a growth factor-regulated protein kinase,[18] suggesting that ERK activation reflects a common pathway of cell responses and is in a position to integrate multiple extracellular signals.

In neural tissues, ERKs are responsive to nerve growth factor,[14] electrical stimulation,[28] and NMDA receptor activation.[29] When activated, ERKs rapidly phosphorylate targets that lead to changes in kinase cascades, protein function, or gene expression. A variety of proteins, including MAP-2, myelin basic protein, tyrosine hydroxylase, retinoblastoma protein, RNA polymerase II, S6 ribosomal protein kinase, and proto-oncogenes including c-*jun* and c-*myc* are readily phosphorylated by ERKs. Analysis of a series of substrates led to the consensus phosphorylation sequence of PX(S/T)P, although in some instances ERKs can phosphorylate (S/T)P motifs.[17,30,31]

Tau is phosphorylated at multiple sites in NFT.[1] Several candidate tau kinases have been proposed,[9–12,32–35] although the biochemical characterization of these kinases is incomplete. Epitope mapping studies suggest that PHF-tau immunoreactivity is due at least in part to phosphorylation of Ser/Thr-Pro motifs.[9,36] Drewes et al[9] and Goedert et al[11] have shown that ERK2 can phosphorylate tau at 14–16 Ser/Thr Pro motifs per molecule. Tau can also be phosphorylated by ERK1[10] and by a novel ATP-sensitive tau kinase that is probably a member of the ERK family.[12] Goedert et al[11] suggest that MAPK (ERK2) co-purifies with PHF,[11] and although we do not detect PHF-associated MAPK immunoreactivity, NFT-bearing neurons are MAPK immunoreactive (Figure 3).[37] Taken together, these observations are consistent with the possibility that ERK2 is responsible for or contributes to the phosphorylation of tau that leads to NFT formation in AD, but of

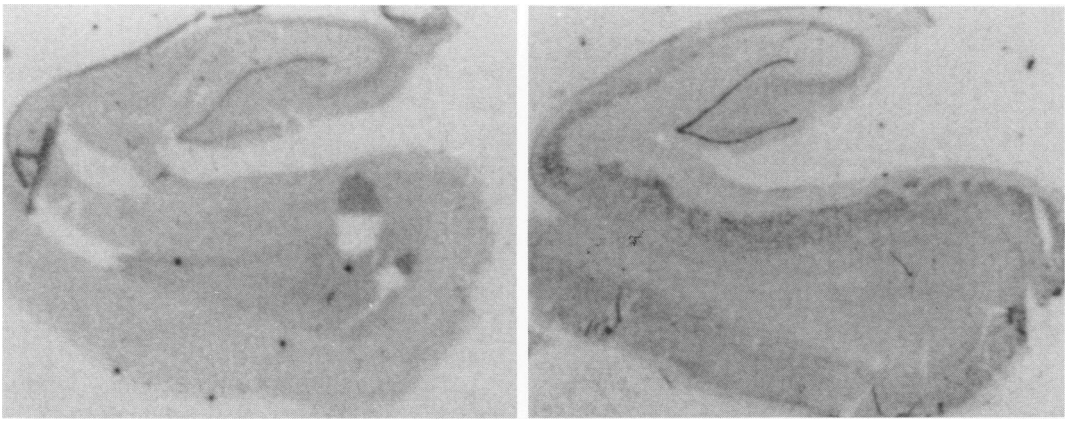

Figure 4. *Autoradiogram of ERK1 (left) and ERK2 (right)* in situ *hybridization in the human hippocampal formation in a 77-year-old control individual. Pretreatment with 10-fold excess unlabeled probe obliterated the signal.*

course there remains the possibility that other kinases are also of critical import.[35]

Our studies show the first neuroanatomical profile of expression of ERK1 and ERK2 and provide for a comparison of this profile to the pattern of NFT changes in AD. The *in situ* hybridization studies suggest that the majority of MAPK immunoreactivity is due to ERK2. The cytoarchitectural fields in the hippocampus that are most intensely MAPK immunoreactive in both controls and individuals with AD are the dentate gyrus granule cells and area CA3, with areas CA1 and the subiculum less strongly stained. Similar conclusions were reached by Trojanowski et al[37] using a different immunoreagent for MAPKs.

The *in situ* hybridization studies suggest that ERK1 is unlikely to be a good candidate for a tau kinase important in AD because it is not located in the appropriate neuroanatomical fields. ERK2 is present in neurons that contain NFT but is also present in many neuronal populations that are fairly resistant to NFT formation (eg, the dentate gyrus granule cells or the lamina principalis interna of the presubiculum). Quantitative *in situ* hybridization studies suggest that the amount of ERK2 message is reduced by approximately 15% in NFT-bearing neurons compared with nearest neighbors that do not contain NFT. However, this reduction is less than the reduction in overall mRNA levels (approximately 25% in our study). These values compare well with a previous study of loss of poly-A mRNA in tangle-bearing neurons, which found a 33% reduction.[38] These results suggests that ERK2 expression is relatively preserved even in the face of substantial metabolic compromise. Also consistent with this interpretation is the measurement using immunoblots that showed an 18% reduction of ERK2 protein in AD hippocampus.[37]

At the immunohistochemical level, no difference was seen in intensity or distribution of MAPK immunostaining in AD. The pattern of NFT in AD differs from that of MAPK staining. Areas CA1 and subiculum are most vulnerable and most severely involved by NFT, with relative sparing of CA3 and the dentate gyrus granule cells, whereas the dentate gyrus granule cells and CA3 neurons are more intensely MAPK immunoreactive than CA1 or subiculum. Similarly, in temporal neocortex the most intensely MAPK-stained neurons are in layers II and VI, moderately positive in layers III and V, and least stained in layer IV. NFT appear most consistently in layers V and III in the inferior temporal gyrus. Our double labeling experiment, however, shows that NFT-bearing neurons do contain MAPK immunoreactivity. This study provides information on the distribution but not on the functional state of MAPKs, so it is possible that MAPKs are more strongly activated in NFT-bearing neurons in AD.

MAPK immunoreactivity is present in neuronal soma and extensive dendritic arborizations, with second- or third-order branch points observed in fortuitous sections. In addition, the axon hillock and proximal axon are clearly immunoreactive in pyramidal neurons. Tau is normally present primarily in axons in neurons and in AD phosphorylated tau accumulates in the neuronal soma and apical and basilar dendrites as NFT and neuritic threads. Thus, MAPKs are present in the same cellular compartments as tau, consistent with the possibility that they contribute to the hyperphosphorylation of tau

associated with NFT formation. However, the anatomical mismatches noted above suggest that expression of MAPKs is not sufficient to predispose neurons toward NFT formation.

Acknowledgments

We thank Sharon Melanson for assistance with manuscript preparation. We thank the Massachusetts Alzheimer Disease Research Center Brain Bank (Dr. E.T. Hedley-Whyte, Director) for tissue samples.

References

1. Goedert M, Sisodia SS, Price DL: Neurofibrillary tangles and b-amyloid deposits in Alzheimer's disease. Curr Opin Neurobiol 1991, 1:441–447
2. Arriagada PV, Growdon JH, Hedley-Whyte ET, Hyman BT: Neurofibrillary tangles but not senile plaques parallel duration and severity of Alzheimer's disease. Neurology 1992, 42:631–639
3. Hagestedt T, Lichtenberg B, Wile H, Mandelkow E-M, Mandelkow E: Tau protein becomes long and stiff upon phosphorylation: correlation between paracrystalline structure and degree of phosphorylation. J Cell Biol 1989, 109:1643–1651
4. Lindwall G, Cole RD: The purification of tau protein and the occurrence of two phosphorylation states of tau in brain. J Biol Chem 1984, 259:12241–12245
5. Baudier J, Cole RD: Phosphorylation of tau proteins to a state like that in Alzheimer's brain is catalyzed by a calcium/calmodulin-dependent kinase and modulated by phospholipids. J Biol Chem 1987, 262:17577–17583
6. Steiner B, Mandelkow E-M, Biernat J, Gustke N, Meyer HE, Schmidt B, Mieskes G, Soling HD, Drechsel D, Kirschner MW, Goedert M, Mandelkow E: Phosphorylation of microtubule-associated protein tau: identification of the site for Ca^{2+}-calmodulin dependent kinase and relationship with tau phosphorylation in Alzheimer tangles EMBO J 1990, 9:3539–3544
7. Hanger DP, Hughes K, Woodgett JR, Brion J-P, Anderton BH: Glycogen synthase kinase-3 induces Alzheimer's disease-like phosphorylation of tau: generation of paired helical filament epitopes and neuronal localization of the kinase. Neurosci Lett 1992, 147:58–62
8. Mandelkow E-M, Drewes G, Biernat J, Gustke N, Van Lint J, Vandenheede JR, Mandelkow E: Glycogen synthase kinase-3 and the Alzheimer-like state of microtubule-associated protein tau. FEBS Lett 1992, 314:315–321
9. Drewes G, Lichtenberg-Kraag B, Doring F, Mandelkow E-M, Biernat J, Goris J, Doree M, Mandelkow E: Mitogen activated protein (MAP) kinase transforms tau protein into an Alzheimer-like state. EMBO J 1992, 11: 2131–2138
10. Ledesma MD, Correas I, Avila J, Diaz-Nido J: Implication of brain cdc2 and MAP2 kinases in the phosphorylation of tau protein in Alzheimer's disease. FEBS Lett 1992, 308:218–224
11. Goedert M, Cohen SE, Jukes R, Cohen P: p42 MAP kinase phosphorylation sites in microtubule associated protein tau are dephosphorylated by protein phosphatase 2A1. FEBS Lett 1992, 312:95–99
12. Roder HM, Schroder W, Eden PA, Ingram VM: PK40, an ATP-sensitive member of ERK-family of kinases, converts TAU protein into PHF-TAU as found in Alzheimer's disease. Soc Neurosci Abstr 1992, 18:561
13. Boulton TG, Yancopoulos GD, Gregory JS, Slaughter C, Moomaw C, Hsu J, Cobb MN: An insulin-stimulated protein kinase similar to yeast kinases involved in cell cycle control. Science 1990, 249:64–66
14. Boulton TG, Nye SH, Robbins DJ, Ip NY, Radziejewska E, Morgenbesser SD, DePinho RA, Panayotatos N, Cobb MH, Yancopoulos GD: ERKs: a family of protein-serine/threonine kinases that are activated and tyrosine phosphorylated in response to insulin and NGF. Cell 1991, 65:663–675
15. Rossomando AJ, Sanghera JS, Marsden LA, Weber MJ, Pelech SL, Sturgill TW: Biochemical characterization of a family of serine/threonine protein kinases regulated by tyrosine and serine/threonine phosphorylation. J Biol Chem 1991, 266:20270–20275
16. Gomez N, Cohen P: Dissection of the protein kinase cascade by which nerve growth factor activates MAP kinases. Nature 1991, 353:170–173
17. Pulverer BJ, Kyriakis JM, Avruch J, Nikolakaki E, Woodgett JR: Phosphorylation of c-*jun* mediated by MAP kinases. Nature 1991, 353:670–674
18. Lange-Carter CA, Pleiman CM, Gardner AM, Blumer KJ, Johnson GL: A divergence in the MAP kinase regulatory network defined by MEK kinase and Raf. Science 1993, 260:315–319
19. Hyman BT, Damasio AR, Van Hoesen GW, Barnes CL: Alzheimer's disease: cell-specific pathology isolates the hippocampal formation. Science 1984, 298:83–95
20. Hyman BT, Van Hoesen GW, Damasio AR: Memory-related neural systems in Alzheimer's disease: an anatomic study. Neurology 1990, 40:1721–1730
21. Roder HM, Eden PA, Ingram VM: Brain protein kinase $PK40^{erk}$ converts TAU into a PHF-like form as found in Alzheimer's disease. Biochem Biophys Res Commun 1993, 193:639–647
22. Rebeck GW, Marzloff K, Hyman BT: The pattern of NADPH-diaphorase staining, a marker of nitric oxide synthase activity, is altered in the perforant pathway terminal zone in Alzheimer's disease. Neurosci Lett 1993, In press
23. Hyman BT, Wenniger JJ, Tanzi RE: Nonisotopic *in situ* hybridization of amyloid precursor protein in Alzheimer's disease: expression in neurofibrillary tangle

bearing neurons and in the microenvironment surrounding senile plaques. Mol Brain Res 1993, 18:253–258
24. Rossomando AJ, Payne DM, Weber MJ, Sturgill TW: Evidence that pp42 a major tyrosine kinase target protein, is a mitogen-activated serine/threonine protein kinase. Proc Natl Acad Sci USA 1989, 86:6940–6943
25. Seger R, Ahn NG, Boulton TG, Yancopoulos GD, Panayotatos N, Radziejewska E, Ericsson L, Bratlien RL, Cobb MH, Krebs EG: Microtubule-associated protein 2 kinases, ERK1 and ERK2, undergo autophosphorylation on both tyrosine and threonine residues: implications for their mechanism of activation. Proc Natl Acad Sci USA 1991, 88:6142–6146
26. Payne DM, Rossomando AJ, Martino P, Erickson AK, Her J-H, Shabanowitz J, Hunt DF, Weber MJ, Sturgill TW: Identification of the regulatory phosphorylation sites in pp42/mitogen-activated protein kinase (MAP kinase). EMBO J 1991, 40:885–892
27. Crews CM, Alessandrini A, Erikson RL: The primary structure of MEK, a protein kinase that phosphorylates the ERK gene product. Science 1992, 258:478–480
28. Stratton KR, Worley PF, Litz JS, Parsons SJ, Huganir RL, Baraban JM: Electroconvulsive treatment induces a rapid and transient increase in tyrosine phosphorylation of a 40-kilodalton protein associated with microtubule-associated protein 2 kinase activity. J Neurochem 1991, 56:147–152
29. Bading PH, Greenberg ME: Stimulation of protein tyrosine phosphorylation by NMDA receptor activation. Science 1991, 253:912–914
30. Clark-Lewis I, Sanghera JS, Pelech SL: Definition of a consensus sequence for peptide substrate recognition by $p44^{mpk}$, the meiosis-activated myelin basic protein kinase. J Biol Chem 1991, 266:15180–15184
31. Alvarez E, Northwood IC, Gonzalez FA, Latour DA, Seth A, Abate C, Curran T, Davis RJ: Pro-leu-Ser/Thr-Pro is a consensus primary sequence for substrate protein phosphorylation. J Biol Chem 1991, 266: 15277–15285
32. Ishiguro K, Takamatsu M, Tomizawa K, Omori A, Takahashi M, Arioka M, Uchida T, Imahori K: Tau protein kinase I converts normal tau protein into A68-like component of paired helical filaments. J Biol Chem 1992, 267:10897–10901
33. Takahashi M, Tomizawa K, Ishiguro K, Sato K, Omori A, Sato S, Shiratsuchi A, Uchida T, Imahori K: A novel brain-specific 25 kDa protein (p25) is phosphorylated by a Ser/Thr-Pro kinase (TPK II) from tau protein kinase fractions. FEBS Lett 1991, 289:37–43
34. Vincent IJ, Davies P: A protein kinase associated with paired helical filaments in Alzheimer disease. Proc Natl Acad Sci USA 1992, 89:2878–2882
35. Biernat J, Gustke N, Drewes G, Mandelkow EM, Mandelkow E: Phosphorylation of ser-262 strongly reduces binding of tau to microtubules: distinction between PHF-like immunoreactivity and microtubule binding. Neuron 1993, 11:153–163
36. Lee VM-Y, Balin BJ, Otvos L, Trojanowski JQ: A68: a major subunit of paired helical filaments and derivatized forms of normal tau. Science 1991, 251:675–678
37. Trojanowski JQ, Mawal-Dewan M, Schmidtt ML, Martin J, Lee VMJ: Localization of the mitogen activated protein kinase ERK2 in Alzheimer disease neurofibrillary tangles and senile plaque neurites. Brain Res 1993, 618:333–337
38. Griffen WST, Ling C, White C, Morrison-Bogorod M: Polyadenylated messenger RNA in paired helical filament immunoreactive neurons in Alzheimer disease. Alzheimer Dis Assoc Disord 1990, 4:69–78